

Advanced Dynamic Algorithms for the Decay of Metastable Phases in Discrete Spin Models: Bridging Disparate Time Scales

M. A. Novotny

Supercomputer Computations Research Institute, Florida State University, Tallahassee, Florida 32306-4130, USA

Received 24 August 1999

Revised 24 August 1999

An overview of advanced dynamical algorithms capable of spanning the widely disparate time scales that govern the decay of metastable phases in discrete spin models is presented. The algorithms discussed include constrained transfer-matrix, Monte Carlo with Absorbing Markov Chains (MCAMC), and projective dynamics (PD) methods. The strengths and weaknesses of each of these algorithms are discussed, with particular emphasis on identifying the parameter regimes (system size, temperature, and field) in which each algorithm works best.

1. Introduction

One of the most challenging hurdles to be overcome before the goal of computational materials design can be realized is the problem of disparate time scales. The time scales range from microscopic (typically an inverse phonon frequency, roughly 10^{-12} s) to the time over which devices made from the materials must operate (years to centuries). The microscopic time scale is much smaller than the time between clock ticks on today's computers, and the times one desires to simulate are much too long to be achieved with traditional algorithms. Consequently, overcoming the hurdle of disparate timescales will require advanced dynamic algorithms which perform faster-than-real-time simulations. Here we briefly review three algorithms that allow such simulations for metastable decay in discrete spin models. Note that since we are interested in the dynamics of the problem, we cannot use advanced algorithms that change the dynamics (such as cluster algorithms, multicanonical algorithms, hybrid Monte Carlo algorithms, etc). Each advanced dynamic algorithm has its strengths and weaknesses, so which one should be used will depend not only on the individual problem to be simulated, but also on the parameter regime in which the problem is to be studied.

We concentrate on applying these advanced dynamical algorithms to the case of metastable decay of the square-lattice Ising model with periodic boundary conditions. This simple model has been used to study the metastable state of nanoscale magnets¹ and the thermal decay of information stored on magnetic recording media². The Hamiltonian is $\mathcal{H} = -J \sum_{\langle i,j \rangle} \sigma_i \sigma_j - H \sum_i \sigma_i$, with the Ising spins $\sigma = \pm 1$. The

first sum is an interaction between nearest neighbors on a square $L \times L$ lattice, and the second sum is the interaction with the external field H . The temperature is taken to be below the critical temperature, $T_c \approx 2.26 \cdots J$. We start with all spins up (equal to +1) and H negative. In addition to the Hamiltonian, the dynamic must be specified: here the dynamic is randomly choosing one of the L^2 spins and deciding whether or not to flip it using a Metropolis flip probability³. One quantity we are interested in is the average lifetime, $\langle \tau \rangle$, before the system reaches some cut-off magnetization (taken to be zero) as it decays to the equilibrium state. Even in this simple model, which decays by homogeneous nucleation and growth, there are different regimes where $\langle \tau \rangle$ has different functional forms⁴. There are four relevant length scales in the problem (far below T_c). Besides L and the lattice spacing, a , these are the critical droplet radius R_c and the typical distance R_o that a supercritical droplet (one with $R > R_c$) grows before it encounters another supercritical droplet. The critical droplet radius for circular droplets is $R_c = \sigma_\infty(T)/2|H|m_{\text{sp}}$ where $\sigma_\infty(T)$ is the surface tension along a primitive lattice vector when $L \rightarrow \infty$, and m_{sp} is the spontaneous magnetization. For the square lattice both $\sigma_\infty(T)$ and m_{sp} are known exactly. The ‘cross-over dynamical phase diagram’ for metastable decay is shown in Fig. 1.

For fields that are too strong the droplet picture of decay is not valid, this is the Strong Field (SF) regime⁴. For weaker fields the nucleation of multiple droplets (MD regime)⁴ leads to decay of the metastable state via an Avrami mechanism⁵ since $R_c \ll R_o \ll L$. A conservative estimate for the ‘mean-field spinodal’ that separates the SF and MD regimes is given by $R_c = a/2$, independent of L . For weak fields and low temperatures a nucleation of a single droplet (SD regime) leads to decay of the metastable state, since $R_c \ll L \ll R_o$. Our estimate⁴ of the ‘dynamic spinodal’ (where $R_o \sim L$) that gives the limit of the SD regime is where the standard deviation of the lifetime is equal to $\langle \tau \rangle/2$. This cross-over depends on system size, and Fig. 1 shows simulation values using 10^3 escapes for $L=10$ and $L=100$. At $|H| > 2J$ and very low temperatures a single overturned spin is the nucleating droplet⁶ and the ‘dynamic spinodal’ for our dynamic is given by⁷ $(4 - H_{\text{DSp}})/T = \frac{3}{2}\ln(L) - 0.82$. Only the last term is an adjustable parameter, which has been chosen to give agreement for L between 8 and 240. For other dynamics, such as sequential updates, the functional form for H_{DSp} is different⁷. The ‘coexistence regime’⁴, with $L < R_c$, is not shown in Fig. 1.

As seen in Fig. 2, $\langle \tau \rangle$, with units of Monte Carlo steps per spin (MCSS), can vary over more than ten orders of magnitude. The remainder of the paper describes briefly the algorithms that allow such simulations to be performed. The data points in Fig. 2 were taken with different techniques described in this paper, including the Monte Carlo with Absorbing Markov Chains (MCAMC) algorithm (with up to $s=3$) and the Projective Dynamics (PD) algorithm with and without a moving wall. With proper use of the algorithms, one obtains the correct lifetimes. Consequently, which points were taken with which algorithms is not in-

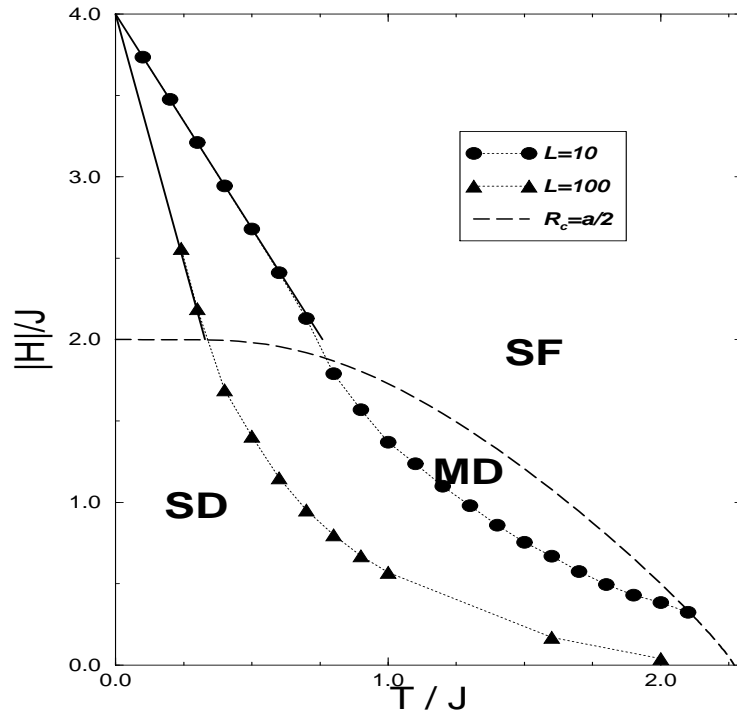


Fig. 1. The ‘cross-over dynamical phase diagram’ for metastable decay of the square-lattice Ising model. The dashed line corresponds to the ‘mean-field spinodal’. The ‘dynamic spinodal’ is shown for $L=10$ and $L=100$. This is a heavy solid line for the analytical expression for $|H| > 2J$, and dotted lines which connect the data points. Shown are the Strong Field (SF), Multi-Droplet (MD), and Single Droplet (SD) decay regimes.

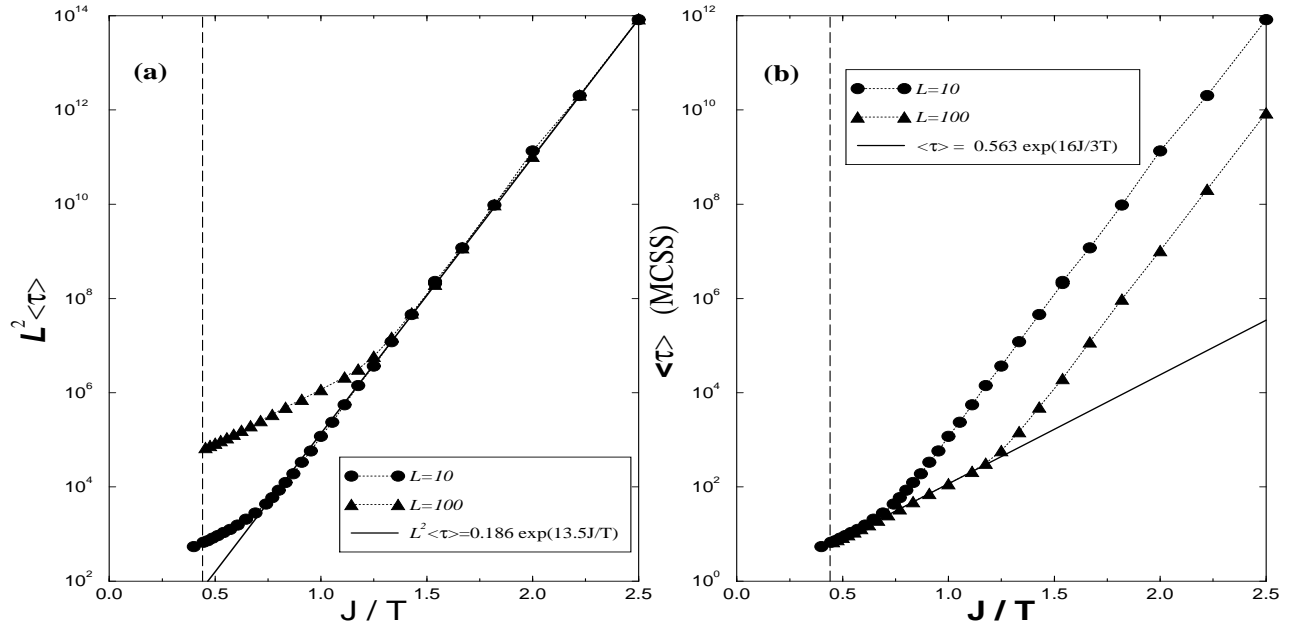


Fig. 2. The average lifetimes, $\langle \tau \rangle$, in units of MCSS, for $L=10$ and $L=100$ are shown as functions of inverse temperature for $H=-0.75J$. The same data are plotted in (a) and (b). The vertical dashed line is J/T_c . In (a) $L^2 \langle \tau \rangle$ is plotted and the data points lie on top of each other in the SD regime. In (b) the same data points lie on top of each other when $\langle \tau \rangle$ is in the MD and SF regimes. The solid lines are from $T \rightarrow 0$ predictions, as described in the text.

licated in the figure. First note that the same data are plotted in parts (a) and (b) of Fig. 2. In the SD regime, Fig. 2(a), the lifetimes for different L lie on top of each other when $L^2\langle\tau\rangle$ is plotted. In the MD regime, Fig. 2(b), the values of $\langle\tau\rangle$ for different L lie on top of each other. The solid lines in Fig. 2 are $T\rightarrow 0$ predictions for the exponential dependence valid for $2/3 \leq |H|/J \leq 1$ from low-temperature predictions^{6,8}. In the SD regime⁶ $\langle\tau\rangle = A_{\text{SD}} \exp[(24J - 14|H|)/T]/L^2$ and in the MD regime⁸ to $\langle\tau\rangle = A_{\text{MD}} \exp[(28J - 16|H|)/3T]$. Only the prefactors are fit to the data. The SD prefactor $A_{\text{SD}} = 0.186$ is set to agree with the data at $T = 0.4J$, while the MD prefactor $A_{\text{MD}} = 0.563$ is set to agree with the $L = 100$ data point at $T = J$.

2. Constrained Transfer Matrix

In the 1960's Langer⁹ used field-theoretical arguments to show that the nucleation rate, and hence the lifetime, can be related to the imaginary part of the analytically continued free energy density, $\mathcal{I}m(\mathcal{F})$. In particular, $\langle\tau\rangle \propto [\mathcal{I}m(\mathcal{F})]^{-1}$. Numerically it is possible to obtain estimates for $\mathcal{I}m(\mathcal{F})$ by finding all eigenvectors and eigenvalues of the $2^\ell \times 2^\ell$ transfer matrix for an $\ell \times \infty$ lattice. This is accomplished by introducing constrained entropy densities¹⁰ in a manner analogous to the source entropy of a stationary ergodic Markov information source. The constrained transfer matrix (CTM) calculations obtain imaginary parts of the free energy density from the imaginary parts of the constrained entropy density. Although the transfer matrix does not contain any explicit dynamics, the CTM method gives $\mathcal{I}m(\mathcal{F})$ values that agree¹⁰ with droplet predictions for the functional form of $\langle\tau\rangle$. It also gives values for metastable magnetizations which agree with those obtained from Avrami analysis of MD growth⁵. Fig. 3 shows the stable and metastable magnetizations from CTM calculations at $|H| = J/2$ for various strip widths ℓ . It illustrates some of the strengths and weaknesses of the CTM method.

- CTM strengths
 - Can obtain $\mathcal{I}m(\mathcal{F})$ directly.
 - Can obtain metastable magnetization easily.
- CTM weaknesses
 - Only feasible for small strip widths. This restricts applications to either mean-field like models or $d=2$ models with short-range interactions.
 - Must use very high precision in the computer calculations.
 - Interpretation subtle because of ‘lobes’ in transfer-matrix spectrum.

3. Monte Carlo with Absorbing Markov Chains

The first algorithm to obtain very large increases in simulated times for faithful dynamics of discrete spin models was put forward about 25 years ago by Bortz, Kalos, and Lebowitz¹¹. This n -fold way method is extremely efficient for low- T

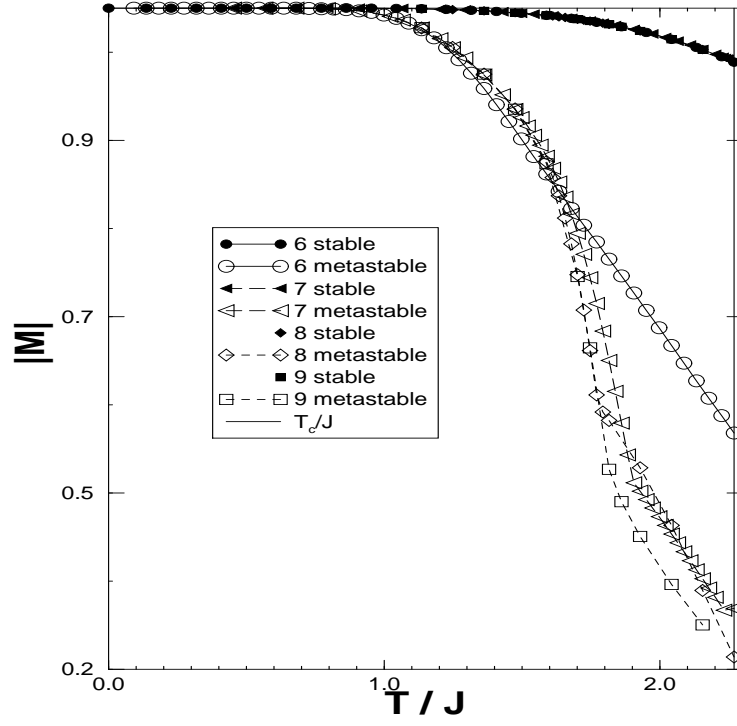


Fig. 3. The absolute values of the stable (closed symbols) and metastable magnetizations (open symbols) at $H=-0.5J$ for $\ell=6, 7, 8, 9$. Note that the crossover between the SD and MD regimes is seen near $T=1.75J$.

simulations. The n -fold way algorithm has been rewritten¹² for the discrete-time algorithm used in this paper, and this version is presented here. The underlying dynamics corresponds to a $2^{L^2} \times 2^{L^2}$ Markov matrix. Since this matrix is too large to diagonalize¹³, we can deal with it one piece at a time within our Monte Carlo simulation. If we look at an $s \times s$ submatrix \mathbf{T} of the original Markov matrix, one has a matrix associated with the absorbing Markov chain (AMC)

$$\mathbf{M} = \begin{pmatrix} \mathbf{I}_{q \times q} & \mathbf{0}_{q \times s} \\ \mathbf{R}_{s \times q} & \mathbf{T}_{s \times s} \end{pmatrix} \quad (3.1)$$

where \mathbf{R} takes into account the q ways to get out of the s states included in the transient matrix \mathbf{T} . Here \mathbf{I} is the identity matrix, and $\mathbf{0}$ is the matrix with all zero elements. The initial vector \vec{v}_I^T (in this section we use the convention common in mathematics where operators act to the left) has zeroes everywhere with the exception of a one in the current spin configuration, which must be one of the s transient configurations. The random time m for exiting from the s transient states is the solution of the equation

$$\vec{v}_I^T \mathbf{T}_{s \times s}^m \vec{e} < r \leq \vec{v}_I^T \mathbf{T}_{s \times s}^{m-1} \vec{e} \quad (3.2)$$

where r is a uniformly distributed random number between 0 and 1, and \vec{e} is the vector with all elements unity. Given that the s transient states are exited at time-step m , the vector of (unnormalized) probabilities to exit to a particular one of the q states is given by

$$\vec{Q}^T = \vec{v}_I^T \mathbf{T}_{s \times s}^{m-1} \mathbf{R}_{s \times q}. \quad (3.3)$$

Once the s transient states have been exited, a new transient subspace is chosen and the algorithm is repeated. It is only Eqns. (3.2) and (3.3) which need to be used to incorporate the methodology of AMC into a Monte Carlo simulation^{14,15}.

For the isotropic square-lattice Ising model in a field, each spin belongs to one of $n=10$ classes. The first 5 classes ($1 \leq i \leq 5$) have spin up and $5-i$ nearest-neighbor spins which are up. The last 5 classes ($6 \leq i \leq 10$) have spin down and $10-i$ nearest-neighbor spins which are up. Let c_i be the number of spins in class i , and let p_i be the probability of flipping a spin in class i given that that particular spin was chosen for a spin-flip attempt.

If $s=1$, only the current spin configuration is in the transient subspace. This corresponds to the discrete-time n -fold way algorithm. In that case, for our square-lattice Ising model, the transient matrix is $\mathbf{T}_{1 \times 1} = 1 - L^{-2} \sum_{i=1}^{10} c_i p_i = 1 - L^{-2} Q_{10}$, which defines Q_{10} . Then Eq. (3.2) becomes $m-1 \leq \ln(r)/\ln(1-L^{-2}Q_{10}) < m$. For $Q_{10} \ll L^2$ the time of exiting can be approximated by¹² $m \approx \Delta t = -L^2 \ln(r)/Q_{10}$ which leads to the continuous-time version of the n -fold way algorithm. The probability of flipping one of the spins in class i is given from Eq. (3.3) by $c_i p_i / Q_{10}$, now independent of m .

- MCAMC strengths

- Can give **MANY** orders of magnitude speed-up, so extremely large lifetimes can be simulated.
- Extremely efficient at low temperatures and small L , *i.e.*, in the SD regime.
- Can have smaller errors in values for $\langle\tau\rangle$ compared with the same number of metastable escapes using normal simulations. This is because the exact average lifetime for exiting from the s transient states is given by $\vec{v}_I^T(\mathbf{I} - \mathbf{T})^{-1}\vec{e}$, which can be incorporated into $\langle\tau\rangle$.
- Can calculate higher moments of the escape time.
- Provides a direct connection between discrete-time Monte Carlo simulations and the continuous time used in the original n -fold way algorithm.
- Can be parallelized in a non-trivial fashion, which has been done for $s=1$ ¹⁶. This allows one to efficiently use multi-processor scalable machines to simulate discrete-event processes on large lattices for long times.
- MCAMC weaknesses
 - Requires tabulation of Markov sub-matrices, which can be complicated for large L or small H .
 - Requires a small number of spins that evolve relatively quickly, so system stays in Markov sub-matrix for a large number of spin flip attempts.
 - Easiest to program efficiently for a small number of spin classes.
 - The parallelized $s=1$ version loses some of its efficiency at low temperatures, compared with the serial algorithm¹⁶.

4. Projective Dynamics

In order to show the similarities between the Projective Dynamics (PD) method^{17,18} and the Transition Matrix Monte Carlo (TMCMC) method¹⁹ we use the TMCMC notation in this section. The dynamics of the single-spin flip process acting on the 2^{L^2} state vector P is given by the continuous-time Markov matrix Γ ,

$$\frac{\partial P(\sigma, t)}{\partial t} = \sum_{\{\sigma'\}} \Gamma(\sigma|\sigma') P(\sigma', t). \quad (4.1)$$

The idea behind both the PD and TMCMC methods is to coarse-grain this process by lumping together some of the 2^{L^2} states according to some variable C . The probability of going from lumped state C to C' is given by

$$W(C|C') = \frac{1}{n(C')} \sum_{\sigma \in \{\sigma|C\}} \sum_{\sigma' \in \{\sigma|C'\}} \Gamma(\sigma|\sigma') \quad (4.2)$$

where $n(C')$ is the number of original states lumped into state C' . This yields

$$\frac{\partial P(C, t)}{\partial t} = \sum_{\{C'\}} W(C|C') P(C', t) \quad (4.3)$$

where $P(C, t)$ is the probability of being in lumped state C at time t . For the PD method we choose $C=M$, so we lump on the magnetization, and since we are interested in metastable decay we work at finite field and temperatures well below T_c . In the TMMC¹⁹ one lumps on the energy, so $C=E$, and one is interested in the critical behavior and works at $H=0$ and temperatures near T_c . One interesting result is that the TMMC method yields dynamics much different¹⁹ from single spin-flip dynamics, due to the allowed ‘microcanonical’ mixing within the lumped states. However, lumping on M does not allow spin flips to occur without jumping out of the current lumped state — and it has been proven that within statistics the correct value of $\langle\tau\rangle$ is obtained²⁰. This means that memory effects due to the lumping in M do not enter into the calculation of $\langle\tau\rangle$. For the PD case, the lumped matrix is tridiagonal and one has $W(M|M')=s(M')\delta_{M+2,M'}+g(M')\delta_{M-2,M'}$ which defines the growing and shrinking rates of the stable phase as $g(M)=\sum_{i=1}^5\langle c_i\rangle_M p_i$ and $s(M)=\sum_{i=6}^{10}\langle c_i\rangle_M p_i$. Here $\langle c_i\rangle_M$ is the average number of spins in class i during the simulated escape given that the configuration has magnetization M .

The random walk starts at $M=L^2$ and terminates at $M=0$. We define $h(M)$ as the total time spent in M . If L is even, $h(M)=0$ for M odd, since these magnetizations are not possible. Then

$$\langle\tau\rangle = \sum_{M=2}^{L^2} h(M), \quad h(M) = \frac{1 + s(M-2)h(M-2)}{g(M)}, \quad h(2) = \frac{1}{g(2)}. \quad (4.4)$$

It is also possible to introduce a moving wall in the magnetization to force the system out of the metastable state, and to measure $g(n)$ and $s(n)$ during this (hopefully quasi-static) process. The wall position is given by $M_{\text{wall}}(t)=(L^2+1)-v_{\text{wall}}t$. For a soft wall the normal Monte Carlo flip probability is multiplied by $p_{\text{wall}}=\exp[-c(M_{\text{new}}-M_{\text{wall}})]$ if the wall at position M_{wall} is past the magnetization of the Monte Carlo new trial configuration. Another possibility is to introduce a hard wall, $c=\infty$, that always flips a chosen up spin if M_{wall} is past the current magnetization. Fig. 4 shows an example of lifetimes for different forcing walls as functions of the wall speed. The difference between the lifetimes measured from Eq. (4.4) and the number of MCSS before escape with the wall gives an estimate for the speed-up due to incorporating the forcing wall. Of course, for a wall moving too fast the process is not quasi-static and the lifetimes are not accurate. However, good results are obtained even for relatively fast walls. For example for the hard wall a velocity of $3\times 10^{-4}M/L^2\text{MCSS}$ gives a lifetime comparable to an actual escape but requires almost two orders of magnitude less computer time. The soft walls do not seem to help the convergence, and additional calculations are needed to calculate p_{wall} . This makes the hard wall more computationally efficient compared with the soft walls.

- PD strengths
 - Can give **MANY** orders of magnitude speed-up, so extremely large lifetimes are possible.

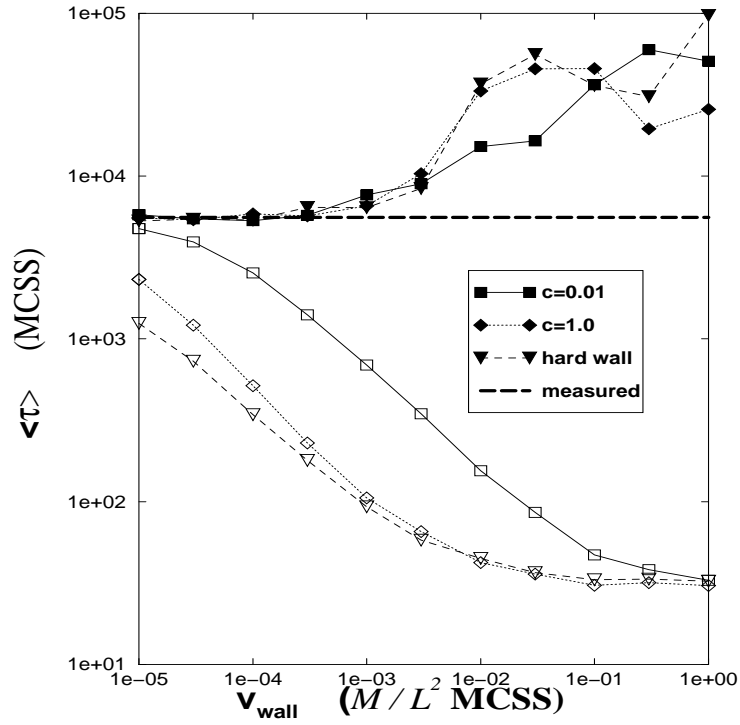


Fig. 4. The average lifetime, $\langle \tau \rangle$, in units of MCSS is shown as a function of the velocity of the forcing wall (in units of $M/L^2 \text{ MCSS}$). This is for a 10×10 lattice with $T=0.9J$ and $H=-0.75J$. The data are for different degrees of softness of the wall, $c=0.01$ (\square), $c=1.0$ (\diamond), and a hard wall $c=\infty$ (∇). The filled symbols are $\langle \tau \rangle$ values from the growing and shrinking probabilities, while the corresponding open symbols are the measured number of MCSS to escape from the metastable state with the forcing wall. The dotted lines connect the data points and serve as guides to the eye. The dashed horizontal line corresponds to the result for $\langle \tau \rangle$ from standard simulations.

- Easy to obtain magnetization of metastable state^{17,21}.
- Easy to obtain magnetization of saddle point^{17,21}.
- Allows extrapolation to very long lifetimes for weak H ¹⁷.
- Allows extrapolation to large L from simulations at smaller L ¹⁷.
- Gives **EXACT** value of lifetime, except for statistical deviations²⁰.
- Has decreased errors in values for $\langle\tau\rangle$ compared with same number of metastable escapes using normal simulations.
- Works well in both SD and MD regimes, as well as the coexistence regime.
- Can incorporate a ‘moving forcing wall’ to further enhance performance¹⁸.
- PD weaknesses
 - Gives only approximate higher moments of lifetime due to memory effects ignored when the states are lumped¹⁷.
 - The original Markov chain is not ‘lumpable’, nor is it even ‘weakly lumpable’¹⁸.
 - It is nontrivial to know how fast to move the wall.

5. Discussion and Conclusions

We have demonstrated several dynamically faithful algorithms to study homogeneous nucleation and growth in discrete spin models. These include the Constrained Transfer Matrix (CTM) method, the Monte Carlo with Absorbing Markov Chains (MCAMC) method which is a generalization of the n -fold way algorithm, and the Projective Dynamics (PD) method. Each method has its own strengths and weaknesses, which are detailed in Sec. 2, 3, and 4, respectively. Consequently, which method should be used depends on the model to be studied and on the parameter regime where the model is to be studied. Application and generalization of these methods to faithfully study the dynamics of other systems, including systems with randomness, continuous spin models²², higher-dimensional systems^{17,18}, and systems evolving via stochastic differential equations are some possible future interesting applications.

Acknowledgments

The author would like to thank M. Kolesik, M.P. Nightingale, P.A. Rikvold, and R.H. Swendsen, for useful discussions. Supported in part by the NSF through grant number DMR-9871455, and through the Supercomputer Computations Research Institute which is funded by the U.S. DOE and the State of Florida. Supercomputer time supplied by National Energy Research Scientific Computing Center (NERSC).

References

1. P. A. Rikvold, M. A. Novotny, M. Kolesik, and H. L. Richards, in *Dynamical Properties of Unconventional Magnetic Systems, NATO Science Series E*, editors A. T. Skjeltorp and D. Sherrington, volume 349, p 307, (Kluwer, Dordrecht, 1998).

2. M. A. Novotny and P. A. Rikvold, in *Encyclopedia of Electrical and Electronics Engineering*, editor J. G. Webster, vol. 12, p. 64, (John Wiley & Sons, New York, 1999).
3. K. Binder and D. Stauffer, in *Applications of the Monte Carlo Method in Statistical Physics*, in *Topics in Current Physics*, Vol. 36, edited by K. Binder (Springer-Verlag, Berlin, 1984).
4. P. A. Rikvold, H. Tomita, S. Miyashita, and S. W. Sides, *Phys. Rev. E* **49**, 5080 (1994).
5. R. A. Ramos, P. A. Rikvold, and M. A. Novotny, *Phys. Rev. B* **59**, 9053 (1999).
6. E. Jordão Neves and R. H. Schonmann, *Commun. Math. Phys.* **137**, 209 (1991); R. Kotecky and E. Olivieri, *J. Stat. Phys.* **70**, 1121 (1993).
7. J. Lee, M. A. Novotny, and P. A. Rikvold, *Phys. Rev. E* **52**, 356 (1995).
8. P. Dehghanpour and R. H. Schonmann, *Commun. Math. Phys.* **188**, 89 (1997).
9. J. S. Langer, *Ann. Phys. (N.Y.)* **41**, 108 (1967); **54**, 258 (1969).
10. C. C. A. Günther, P. A. Rikvold, and M. A. Novotny, *Phys. Rev. Lett.* **71**, 3898 (1993); *Physica A* **212**, 194 (1994); and references therein.
11. A. B. Bortz, M. H. Kalos, and J. L. Lebowitz, *J. Comput. Phys.* **17**, 10 (1975).
12. M. A. Novotny, *Computers in Physics* **9**, 46 (1995).
13. See the article by M. P. Nightingale, *Int. J. Mod. Phys. C*, this volume.
14. M. A. Novotny in *Computer Simulations in Condensed Matter Physics VII* editors D. P. Landau, K. K. Mon, and H.-B. Schüttler, p. 161 (Springer-Verlag, Heidelberg, 1994).
15. M. A. Novotny, *Phys. Rev. Lett.* **74**, 1 (1995); erratum **75**, 1424 (1995).
16. G. Korniss, M. A. Novotny, and P. A. Rikvold, *J. Comput. Phys.* **153**, 488 (1999).
17. M. Kolesik, M. A. Novotny, P. A. Rikvold, and D. M. Townsley, in *Computer Simulations in Condensed Matter Physics X*, editors D. P. Landau, K. K. Mon, and H.-B. Schüttler, p. 246 (Springer-Verlag, Heidelberg, 1998).
18. M. Kolesik, M. A. Novotny, and P. A. Rikvold, *Phys. Rev. Lett.* **80**, 3384 (1998).
19. J.-S. Wang, T. K. Tay, and R. H. Swendsen, *Phys. Rev. Lett.* **82**, 476 (1999); R. H. Swendsen, *Int. J. Mod. Phys. C*, this volume.
20. M. A. Novotny, M. Kolesik, and P. A. Rikvold, *Computer Phys. Commun.* preprint cond-mat/9811039, in press (1999).
21. M. Kolesik, M. A. Novotny, and P. A. Rikvold, *Mat. Res. Soc. Symp. Proc.* **492**, 313 (1998).
22. S. J. Mitchell, M. A. Novotny, and J. D. Munoz, *Int. J. Mod. Phys. C*, this volume.